

PERFORMANCE OF RECEIVERS IN DIGITAL RADIO APPLICATIONS
OPERATING IN THE PRESENCE OF NOISE AND JAMMING

Daniel C. Bukofzer

Department of Electrical and Computer Engineering
Naval Postgraduate School, Code 62 Bh
Monterey, California 93943

ABSTRACT

The performance of digital communication systems operating in the presence of noise and jamming is analyzed and evaluated. Specifically, by modeling the jamming as additive colored Gaussian noise, and considering transmission via M-ary phase shift keyed (MPSK) modulation as well as Quadrature Amplitude Modulation (QAM), receiver performance is determined in terms of symbol error probability, P_s . The receiver analyzed is optimum for the modulation used when the channel interference consists of additive white Gaussian noise (AWGN) only, and does not process signals utilizing spread spectrum modulation or forward error correction schemes. Furthermore, the derived results for P_s are used in order to optimize the shape of the colored noise (jamming) spectrum so as to cause maximum receiver degradation, subject to a jamming power constraint. Results on numerical evaluations are presented graphically, thus displaying receiver vulnerability to a specific form of jamming.

INTRODUCTION

The performance of communication systems operating in the presence of jamming has received a great deal of attention in the recent past. Most analyses have concentrated on the performance of complex digital communication systems having both spread spectrum modulation and forward error correcting capabilities. Such systems exhibit good jam resistance, however can be quite difficult to implement and operate at theoretically predicted performance levels. Still, many communication systems continue to be operated with no spread spectrum modulation and/or forward error correction capabilities. The question that naturally arises is, how vulnerable to jamming are such systems. This issue is addressed here by considering an important class of digital communication systems operating in the presence of noise and jamming using an additive colored noise model for the jammer (as opposed to barrage white noise jamming). Furthermore, it is demonstrated that it is possible to optimally shape the colored noise spectrum so as to cause maximum degradation on the performance of the digital communication system.

In the first section of this paper, the signal, noise and jamming models are introduced. The second section presents an analysis of the performance of an M-ary Phase Shift Keyed (MPSK) modulation receiver operating in the presence of

noise and jamming. A mathematical expression for P_s , the receiver symbol error probability, is derived and used to obtain an optimum colored noise (jamming) spectrum, so as to cause maximum receiver degradation, subject to a jamming power constraint. The same analysis is then carried out in the third section for a Quadrature Amplitude Modulation (QAM) receiver operating in the presence of noise and jamming. The derivation of the receiver symbol error probability is followed by a solution to the corresponding jammer optimization problem. The fourth section presents graphical results involving plots of receiver error probability as a function of signal-to-noise ratio and jamming-to-signal ratio. Following an interpretation of the results, concluding remarks are presented.

SIGNAL, NOISE, AND JAMMING MODELS

We assume that one of M signals $s_i(t)$, $i = 1, 2, \dots, M$ is transmitted over the interval $0 \leq t \leq T_s$. The channel noise is modeled as additive White Gaussian (AWGN), having power spectral density (PSD) level $N_0/2$. The signal $j(t)$ produced by the jammer will be modeled as additive colored Gaussian noise as of yet, unspecified spectral density shape, $S_j(f)$. We will only require a jamming power constraint, that is

$$\int_{-\infty}^{\infty} S_j(f) df \triangleq P_j < \infty \quad (1)$$

Thus, the received signal $r(t)$ can be mathematically expressed as

$$r(t) = s_i(t) + n(t) + j(t) \quad i=1,2,\dots,M; \quad 0 \leq t \leq T_s \quad (2)$$

and, for the signal modulation schemes to be considered, a representation

$$s_i(t) = \sum_{k=1}^2 S_{ik} \phi_k(t) \quad i=1,2,\dots,M; \quad 0 \leq t \leq T_s \quad (3)$$

in terms of a complete orthonormal (C.O.N.) set of functions $\{\phi_k(t)\}$ is possible. The components $\{S_{ik}\}$ for $i=1,2,\dots,M$ are obtained from

$$S_{ik} = \int_0^{T_s} s_i(t) \phi_k(t) dt \quad i=1,2,\dots,M; \quad k=1,2 \quad (4)$$

If each signal $s_i(t)$ of energy E_i , $i=1,2,\dots,M$ is equally likely to be transmitted, and $j(t)=0$, the conceptual structure of the optimum receiver is

well-known (ref. 1), as demonstrated in Figure 1. The analysis in the sequel establishes the performance of this receiver where $j(t) \neq 0$, for specific signal modulations, namely M-ary Phase Shift Keyed (MPSK) modulation, and Quadrature Amplitude Modulation (QAM). Additionally, it will be demonstrated that an optimum solution for the (colored) jamming PSD $S_j(f)$ is possible, subject to a power constraint as specified in eq. 1.

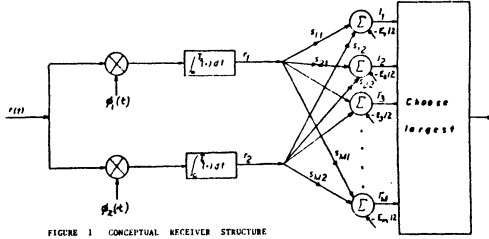


FIGURE 1 CONCEPTUAL RECEIVER STRUCTURE

RECEIVER ERROR PROBABILITY FOR MPSK MODULATION

The signal model for MPSK is

$$s_i(t) = \sqrt{\frac{2E_s}{T_s}} \cos(2\pi f_0 t + \frac{2\pi(i-1)}{M} + \alpha) \quad (5)$$

for $i = 1, 2, \dots, M$; $0 \leq t \leq T_s$, where α is an arbitrary, yet fixed phase. Since all signals $s_i(t)$, $i = 1, 2, \dots, M$ have the same energy, that is

$$E_i = \int_0^{T_s} s_i^2(t) dt = E_s \quad i = 1, 2, \dots, M \quad (6)$$

it is clear that the receiver of Figure 1 simplifies somewhat in that determination of l_i' only, where

$$l_i' = \sum_{k=1}^2 r_k s_{ik} \quad i = 1, 2, \dots, M \quad (7)$$

is necessary. From trigonometric expansion of eq. 5, we have

$$\phi_1(t) = \frac{\cos(2\pi f_0 t + \alpha)}{\sqrt{T_s/2}}; \phi_2(t) = \frac{\sin(2\pi f_0 t + \alpha)}{\sqrt{T_s/2}} \quad (8)$$

for $0 \leq t \leq T_s$, and,

$$s_{i1} = \sqrt{E_s} \cos \frac{2\pi(i-1)}{M} \quad s_{i2} = -\sqrt{E_s} \sin \frac{2\pi(i-1)}{M} \quad (9)$$

for $i = 1, 2, \dots, M$ where it has been assumed for convenience that $2f_0 T_s$ is an integer. Thus, eq. 7 can be put in the form

$$l_i' = v \cos(\theta_i + \eta) \quad i = 1, 2, \dots, M \quad (10)$$

where

$$v^2 = \sum_{k=1}^2 r_k'^2; \eta = \tan^{-1} \frac{r_2'}{r_1'} \quad (11)$$

and,

$$r_k' = \sqrt{E_s} r_k = \sqrt{E_s} \int_0^{T_s} r(t) \phi_k(t) dt, \quad k = 1, 2;$$

$$\theta_i = \frac{2\pi(i-1)}{M}, \quad i = 1, 2, \dots, M \quad (12)$$

If the signal $s_m(t)$ is transmitted, the probability of a correct decision, denoted $\Pr\{C/m\}$ is obtained from

$$\Pr\{C/m\} = \Pr\{l_m' > l_i'; \forall i \neq m\} \quad (13)$$

Since $n(t)$ and $j(t)$ are zero mean, statistically independent random processes, the joint probability specified by eq. 13 can be determined. As a preliminary, observe that

$$E\{r_k'/s_m(t) \text{ transmitted}\} \triangleq \mu_{km} = \sqrt{E_s} s_{mk} \quad (14)$$

for $k=1, 2$ and

$$E\{(r_1' - \mu_{1m})(r_2' - \mu_{2m})/s_m(t) \text{ transmitted}\} = \int_0^T \int_0^T (K_n(t-T) + K_j(t-T)) \phi_1(t) \phi_2(T) dt dT \quad (15)$$

where $K_n(\cdot)$ and $K_j(\cdot)$ are the noise and jammer

autocorrelation functions respectively. It is shown in the appendix that the integral of eq. 15 is zero and furthermore

$$\text{var}\{r_k'/s_m(t) \text{ transmitted}\} \triangleq \sigma_{km}^2 = \frac{N_0}{2} + \int_0^T \int_0^T K_j(t-T) \phi_k(t) \phi_k(T) dt dT \quad (16)$$

for $k = 1, 2$

Thus r_1' and r_2' are independent Gaussian r.v.'s

Since eq. 16 is independent of the index m , and as demonstrated in the appendix, also independent of the index k , the joint probability density function (p.d.f.) of r_1' and r_2' can be easily obtained. From such p.d.f. and the relationship specified in eq. 11, it can be demonstrated that

$$f_{\eta}/s_m(t) \quad (V, H) = \frac{V}{\sqrt{(2\pi)^2 \sigma^2}} \exp \left\{ \frac{-1}{2\sigma^2} (V^2 + E_s - 2V\sqrt{E_s} \cos(\theta_m + H)) \right\} \quad \begin{matrix} V \geq 0 \\ 0 \leq H \leq 2\pi \end{matrix} \quad (17)$$

where

$$\sigma^2 = \frac{N_0}{2} + \frac{J_0}{2} \quad (18)$$

and

$$J_0 = \int_0^T \int_0^T K_j(t-T) \phi_k(t) \phi_k(T) dt dT \quad (19)$$

for $k = 1$ or 2 ,

The desired p.d.f. of η is obtained implicitly via integration of eq. 17 over the r.v. v through its range $(0, \infty)$. A number of tedious steps are

required to demonstrate that

$$f_{\eta/s_m}(t) (H) = \frac{1}{2\pi} \exp\left\{\frac{-E_s}{2\sigma^2}\right\} + \sqrt{\frac{2\pi E_s}{\sigma^2}} \cos(\theta_m + H) \operatorname{erf}_* \left\{ \frac{\sqrt{E_s} \cos(\theta_m + H)}{\sigma} \right\} \quad (20)$$

where $\operatorname{erf}_*(\cdot)$ is the error function, as defined in ref. 2. From eq. 10, due to the behavior of the cosine function, it can be demonstrated that eq. 13 can be evaluated as

$$\Pr\{C/m\} = \int_{-\theta_m - \pi/M}^{-\theta_m + \pi/M} f_{\eta/s_m}(t) (H) dH = \frac{1}{M} e^{-E_s/2\sigma^2} + \int_{-\pi/M}^{\pi/M} \sqrt{\frac{E_s}{2\pi\sigma^2}} (\cos\beta) e^{-E_s \sin^2 \beta / 2\sigma^2} \operatorname{erf}_* \left\{ \frac{\sqrt{E_s} \cos\beta}{\sigma} \right\} d\beta \quad (21)$$

Since eq. 21 is independent of the index m , as expected, and the signals are equally likely to be transmitted.

$$P_s = 1 - \Pr\{C\} = 1 - \Pr\{C/m\} \quad (22)$$

where $\Pr\{C/m\}$ is given either by eq. 21, or by an equivalent expression, namely

$$\Pr\{C/m\} = 2 \int_0^{\infty} \frac{1}{\sqrt{2\pi}} \exp\left\{\frac{-1}{2}(u - R_D)^2\right\} \int_0^u \frac{1}{\sqrt{2\pi}} e^{-v^2/2} dv du = \Pr\{C\} \quad (23)$$

In eq. 23, R_D is defined by

$$R_D = \frac{R_d}{1 + R_j R_d}; \quad R_d = \frac{E_s}{N_o/2} \triangleq \text{signal-to-noise ratio} \quad (24)$$

and

$$R_j = \frac{J_o/2}{E_s} \triangleq \text{jamming power-to-signal energy ratio} \quad (25)$$

Jammer optimization can now be carried out by first evaluating

$$\frac{\partial}{\partial R_j} \Pr\{C\} = -\frac{1}{2} \sqrt{\frac{R_D}{2}} \int_{R_D/2}^{\infty} \operatorname{erf}_* \left\{ (\sqrt{2x} + \sqrt{R_D}) \tan \frac{\pi}{M} \right\} e^{-x} dx < 0 \quad (26)$$

and thus demonstrating that P_s is monotonically

increasing in R_j . Therefore, maximization of P_s requires that for fixed E_s , R_j be made as large as possible. However, since

$$R_j = \frac{J_o}{2E_s} = \frac{1}{E_s} \int_{-\infty}^{\infty} S_j(f) |\phi_1'(f)|^2 df = \frac{1}{E_s} \int_{-\infty}^{\infty} S_j(f) |\phi_2'(f)|^2 df \quad (27)$$

the Cauchy-Schwarz inequality yields

$$R_j \leq \frac{1}{E_s} \left[\int_{-\infty}^{\infty} S_j^2(f) df \int_{-\infty}^{\infty} |\phi_1'(f)|^4 df \right]^{1/2} \quad (28)$$

with equality if and only if

$$S_j(f) = \gamma |\phi_1'(f)|^2 \quad (29)$$

The constant of proportionality γ can be set so as to satisfy the power constraint of eq. 1, so that the optimum PSD choice is given by

$$S_j(f) = P_j |\phi_1'(f)|^2 / \int_{-\infty}^{\infty} |\phi_1'(f)|^2 df \quad (30)$$

resulting in

$$(R_j)_{\text{opt}} = |\phi_1'(f)|^2 / \frac{E_s}{P_j} \int_{-\infty}^{\infty} |\phi_1'(f)|^2 df \quad (31)$$

It is possible to evaluate $(R_j)_{\text{opt}}$ utilizing eqs.

A-5 and A-11, so that eq. 31 becomes (ref.3) $(R_j)_{\text{opt}} = \frac{P_j T_s}{3E_s} = \text{jamming energy-to-signal energy ratio.}$ (32)

RECEIVER ERROR PROBABILITY FOR QAM

The signal model for QAM is

$$s_i(t) = a_{m_{1i}}(t) \cos(2\pi f_o t + \alpha) + a_{m_{2i}}(t) \sin(2\pi f_o t + \alpha) \quad (33)$$

for $i=1, 2, \dots, M$ and $0 \leq t \leq T_s$, and

$$m_{1i}(t) = \begin{cases} \pm 1, \pm 3 \text{ for 16 QAM} \\ \pm 1, \pm 3, \pm 5, \pm 7 \text{ for 64 QAM} \\ \pm 1, \pm 3, \pm 5, \pm 7, \pm 9, \pm 11, \pm 13, \pm 15 \text{ for 256 QAM} \end{cases} \quad (34)$$

$$m_{2i}(t) = \begin{cases} \pm 1, \pm 3 \text{ for 16 QAM} \\ \pm 1, \pm 3, \pm 5, \pm 7 \text{ for 64 QAM} \\ \pm 1, \pm 3, \pm 5, \pm 7, \pm 9, \pm 11, \pm 13, \pm 15 \text{ for 256 QAM} \end{cases} \quad (35)$$

The waveforms $m_{1i}(t)$ and $m_{2i}(t)$ are defined over $0 \leq t \leq T_s$, so that the signal representation in the form of eq. (3) is applicable here with $\phi_1(t)$ and $\phi_2(t)$ given by eq. (8) and

$$S_{i1} = A m_{1i} \quad S_{i2} = A m_{2i} \quad A = a \sqrt{T_s/2} \quad (36)$$

In eq. 36, m_{1i} and m_{2i} take on the constant

values specified by eqs. 34 and 35. The receiver of Figure 1 can be used to recover the digital information, however, in practice, the actual receiver implementation can take advantage of the signal structure in order to simplify its decision mechanism. For 16 QAM, the receiver of Figure 2 is equivalent to that of Figure 1, while the analysis of the performance of the former is considerably simpler than the latter. For 64 QAM and 256 QAM schemes, the basic structure of the receiver in Figure 2 remains unchanged, while only the decision logic mechanism must be modified appropriately.

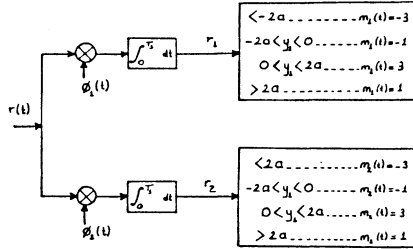


FIGURE 2 RECEIVER STRUCTURE FOR QAM

Assume now that $s_m(t)$ is transmitted. Thus,

$$r(t) = \sum_{k=1}^2 S_{mk} \phi_k(t) + n(t) + j(t) \quad 0 \leq t \leq T_s \quad (37)$$

so that

$$r_k = S_{mk} + N_k + j_k \quad k = 1, 2 \quad (38)$$

where

$$N_k = \int_0^{T_s} n(t) \phi_k(t) dt; j_k = \int_0^{T_s} j(t) \phi_k(t) dt \quad k=1, 2 \quad (39)$$

Clearly, r_k is a Gaussian r.v. for which we can obtain

$$E\{r_k/s_m(t) \text{ transmitted}\} = S_{mk} \quad k = 1, 2 \quad (40)$$

$$E\{(r_1 - S_{m1})(r_2 - S_{m2})/s_m(t) \text{ transmitted}\} \\ = E\{(n_1 + j_1)(n_2 + j_2)\} \quad (41)$$

Due to the independence of the noise and the jamming, a close analysis of eq. 41 reveals that it is identical to eq. 15. Therefore r_1 and r_2 are again uncorrelated r.v.'s with

$$\text{var}\{r_k/s_m(t) \text{ transmitted}\} = \frac{N_0}{2} + \int_0^{T_s} \int_0^{T_s}$$

$$K_j(t - \tau) \phi_k(t) \phi_k(\tau) dt d\tau \quad k = 1, 2 \quad (42)$$

Using the notation introduced in eqs. 18 and 19, we obtain the p.d.f.

$$f_{r_1 r_2 / s_m(t)}(R_1, R_2) = \frac{1}{\sqrt{2\pi\sigma^2}} e^{-(R_1 - S_{m1})^2 / 2\sigma^2} \\ \frac{1}{\sqrt{2\pi\sigma^2}} e^{-(R_2 - S_{m2})^2 / 2\sigma^2} \quad (43)$$

so that

$$\Pr\{C/m\} = \int_{L_{m1}}^{L_{mu}^1} \int_{L_{m1}}^{L_{mu}^2} f_{r_1 r_2 / s_m(t)}(R_1, R_2) dR_1 dR_2 \quad (44)$$

where the integration limits in eq. 44 are now dependent on the particular transmitted signal. Thus, eq. 44 becomes

$$\Pr\{C/m\} = \int_{g_{m1}}^{g_{mu}} \frac{1}{\sqrt{2\pi}} e^{-z^2/2} dz \int_{h_{m1}}^{h_{mu}} \frac{1}{\sqrt{2\pi}} e^{-w^2/2} dw \quad (45)$$

where

$$h_{m1} = (L_{m1}^2 - S_{m2})/\sigma \quad h_{mu} = (L_{mu}^2 - S_{m2})/\sigma \quad (46)$$

$$g_{m1} = (L_{m1}^1 - S_{m1})/\sigma \quad g_{mu} = (L_{mu}^1 - S_{m1})/\sigma$$

Specific evaluation of eq. 45 requires that all possible transmitted signals be considered. This procedure is tedious, however due to signal symmetry, it is possible to evaluate $\Pr\{C\}$ for any QAM scheme. It can be shown that regardless of QAM scheme considered, there are four signals for which

$$\Pr\{C/m\} = \{\text{erf}_*(A/\sigma)\}^2 \quad (47)$$

For 16 QAM there are 8 signals for which

$$\Pr\{C/m\} = \text{erf}_*(A/\sigma) \{1 - 2\text{erfc}_*(A/\sigma)\} \quad (48)$$

For 64 QAM there are 24 signals for which $\Pr\{C/m\}$ is given by eq. 48, while for 256 QAM, there are 56 such signals. Finally, for 16 QAM, 4 signals have

$$\Pr\{C/m\} = \{1 - 2\text{erfc}_*(A/\sigma)\}^2 \quad (49)$$

while for 64 QAM and 256 QAM, there are respectively 36 and 196 such signals. Introducing now the definition

$$d \triangleq \frac{A}{\sigma} = \left[\frac{R_d}{10(1 + R_d R_j)} \right]^{1/2} \quad (50)$$

where R_d and R_j are defined by eq. 24, we obtain for 16 QAM,

$$\Pr\{C\} = \frac{1}{16} \sum_{m=1}^{16} \Pr\{C/m\} = \frac{1}{4} \left[\{\text{erf}_*(d)\}^2 + 2\text{erf}_*(d) \{1 - 2\text{erfc}_*(d)\} + \{1 - 2\text{erfc}_*(d)\}^2 \right] \quad (51)$$

The meaning of E_s in the definition of R_j must now be modified to imply average signal set energy, that is

$$E_s = \frac{1}{M} \sum_{i=1}^M E_i \quad (52)$$

An expression similar to eq. 51 can be obtained for 64 QAM and 256 QAM, except that a modification must be made to account for the corresponding greater number of signals.

Jammer optimization can now be carried out by first evaluating

$$\frac{\partial}{\partial d} P_s = - \frac{3}{2\sqrt{2\pi}} \exp \left\{ -\frac{d^2}{2} \right\} [1 - 3\text{erf}_*(d)] \leq 0 \quad (53)$$

where $P_s = 1 - \Pr\{C\}$. This demonstrates that P_s is monotonically decreasing in d while from eq. 50, d is monotonically decreasing in R_j . Thus for fixed E_s , P_s is maximized by maximizing R_j . Consequently, the derivations presented in eqs. 28 through 32 are applicable here, so that a specification of the optimum jamming spectrum is now available. The details of the derivations of eqs. 47 through 49 can be found in ref. 4. Specific results for 64 QAM and 256 QAM as well as a corresponding proof of the monotonicity of P_s can be found in ref. 4.

GRAPHICAL RESULTS

In this last section, performance plots are presented for both the MPSK and QAM receivers analyzed in Sections II and III respectively. All plots display P_s as a function of signal-to-noise ratio, (SNR), for different values of jamming-to-signal ratio, (JSR), and include a performance curve for the $j(t) = 0$ case. This allows a determination of jammer effectiveness for the different cases considered. Figures 3, 4, and 5 present results for 4 PSK (also known as QPSK), 8 PSK, and 16 PSK respectively. In all cases, the jammer effectiveness can be confirmed from the fact that large SNR penalties result even at such low JSR values as 10dB.

From a comparison stand point, the performance penalties for QAM are not as severe as those for MPSK. This can be observed from Figures 6, 7, and 8. Specifically, Figure 6 can be contrasted with Figure 5, so as to observe the smaller SNR penalty for 16 QAM than in 16 PSK, at a JSR value of (for instance)-20dB. However, it can be observed that the jamming considered is still quite effective insofar as performance degradation of the QAM receiver is concerned.

It can be therefore concluded that an optimized additive colored Gaussian noise jammer, even at low JSR values can effectively degrade digital signal transmission via MPSK and QAM schemes. While these two methods are not the only ones used in digital radio applications, they represent an important class of modulation schemes. Other methods, such as coherent and non-coherent M-ary Frequency Shift Keyed modulation have been analyzed, and the results reported on in ref. 6. It must

however be remembered that the receivers analyzed have no jamming protection, and therefore exhibit the performance behavior described graphically by the figures. The effectiveness of the jamming considered against similar systems employing spread spectrum modulation and forward error correction techniques has not yet been determined.

APPENDIX

We analyze here eq. 15, which becomes

$$\begin{aligned} & \int_0^T \int_0^T \frac{N_o}{2} \delta(t-\tau) \phi_1(t) \phi_2(\tau) dt d\tau + \\ & \int_0^T \int_0^T K_j(t-\tau) \phi_1(t) \phi_2(\tau) dt d\tau = \frac{N_o}{2} \int_0^{T_s} \phi_1(t) \phi_2(t) dt + \\ & \int_{-\infty}^{\infty} S_j(f) \phi_1'(f) (-f) \phi_2'(f) df \end{aligned} \quad (A-1)$$

where the Fourier Transform pairs are

$$K_j(t) \longleftrightarrow S_j(f) \quad (A-2)$$

$$\phi_k'(t) \longleftrightarrow \phi_k'(f) \quad k=1,2 \quad (A-3)$$

where

$$\begin{aligned} \phi_1'(t) &= p(t) \cos(2\pi f_o t + \alpha) \\ p(t) &= \sqrt{\frac{2}{E_s}} \quad 0 \leq t \leq T_s \\ \phi_2'(t) &= p(t) \sin(2\pi f_o t + \alpha) \end{aligned} \quad (A-4)$$

Without loss of generality, in order to simplify the notation we set $\alpha=0$. Observe that the single integral in t of eq. A-1 is zero.

Also

$$p(t) \longleftrightarrow P(f) = \sqrt{2T_s} e^{-j\pi f T_s} \text{sinc} f T_s \quad (A-5)$$

so that

$$\phi_1'(f) = \frac{1}{2} [P(f-f_o) + P(f+f_o)] \quad (A-6)$$

$$\phi_2'(f) = \frac{1}{2j} [P(f-f_o) - P(f+f_o)] \quad (A-7)$$

Now, forming the product $\phi_1'(-f) \phi_2'(f)$, we obtain

$$\begin{aligned} \phi_1'(-f) \phi_2'(f) &= \frac{T_s}{4j} \left[(e^{j2\pi f_o T_s} - e^{-j2\pi f_o T_s}) \text{sinc}(f+f_o) T_s \right. \\ & \quad \left. \text{sinc}(f-f_o) T_s + \text{sinc}^2(f-f_o) T_s - \right. \end{aligned}$$

$$\text{sinc}^2(f+f_o)T_s \Big] \quad (\text{A-8})$$

For realistic values of the parameters f_o and T_s , we observe that

$$\text{sinc}(f+f_o)T_s \text{ sinc}(f-f_o)T_s \simeq 0 \quad (\text{A-9})$$

and furthermore

$$\text{sinc}^2(f-f_o)T_s - \text{sinc}^2(f+f_o)T_s = - [\text{sinc}^2(-f-f_o)T_s - \text{sinc}^2(-f+f_o)T_s] \quad (\text{A-10})$$

demonstrating that $\text{sinc}^2(f-f_o)T_s - \text{sinc}^2(f+f_o)T_s$ is an odd function of f .

Since $S_j(f)$ is an even function of f , we observe that the single integral in f of eq. A-1 also is zero. From the foregoing we observe that

$$\begin{aligned} |\phi_1'(f)|^2 &\simeq \frac{1}{4} \{ |P(f-f_o)|^2 + |P(f+f_o)|^2 \} \\ &\simeq |\phi_2'(f)|^2 \end{aligned} \quad (\text{A-11})$$

so that

$$|\phi_2'(f)|^2 \simeq |\phi_1'(f)|^2 \quad (\text{A-12})$$

thus demonstrating that

$$\begin{aligned} \int_{-\infty}^{\infty} S_j(f) \phi_1'(-f) \phi_1'(f) df &\simeq \\ \int_{-\infty}^{\infty} S_j(f) \phi_2'(f) \phi_2'(-f) df \end{aligned} \quad (\text{A-13})$$

REFERENCES

- (1) Wozencraft, J. and Jacobs, I., "Principles of Communication Engineering", John Wiley 1965
- (2) Van Trees, H. L., "Detection, Estimation, and Modulation Theory," Part I, John Wiley 1968, pp. 37.
- (3) Gradshteyn, I. S., and Ryzhik, I. M., "Table of Integrals, Series, and Products," Academic Press 1965, pp. 446-450.
- (4) Gunes, F., "Performance of Modified M-ary PSK and QAM Signaling Schemes in the Presence of Noise and Jamming," M.S. Thesis, Naval Postgraduate School, June 1986.
- (5) Shoop, B., "Analysis of Digital Receiver Performance in a Jamming Environment for Phase Coherent, Differentially Coherent, and Quadrature Amplitude Modulations," M.S. Thesis, Naval Postgraduate School, Monterey, Calif., Sept. 1986.
- (6) Munoz, L., "Jamming Effects on M-ary Coherent and Binary Noncoherent Digital Receivers Using Random Jammer Models," M.S. Thesis, Naval Postgraduate School, Monterey, Calif., Dec. 1985.

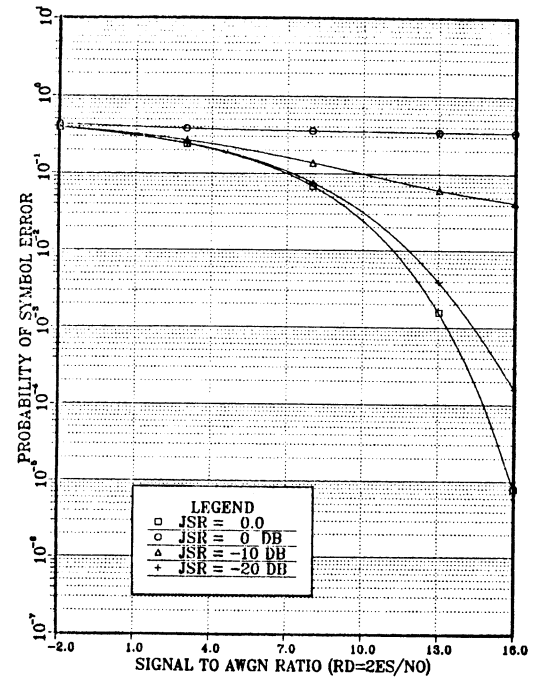


FIGURE 3 QPSK PERFORMANCE IN JAMMING

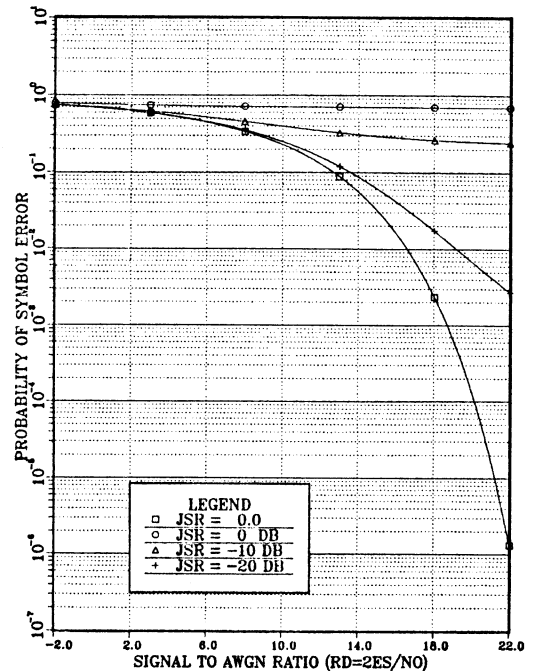


FIGURE 4 8-PSK PERFORMANCE IN JAMMING

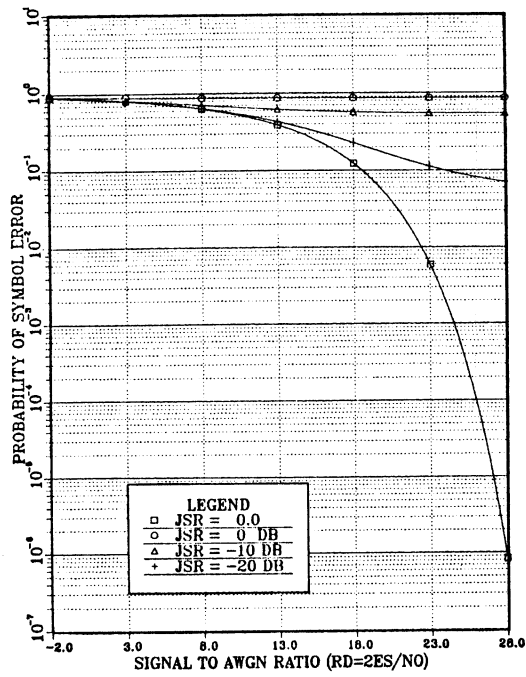


FIGURE 5 16-PSK PERFORMANCE IN JAMMING

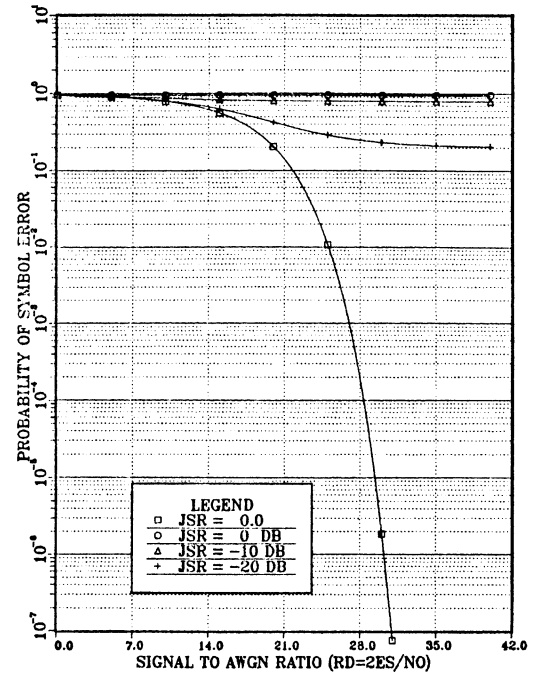


FIGURE 7 64-QAM PERFORMANCE IN JAMMING

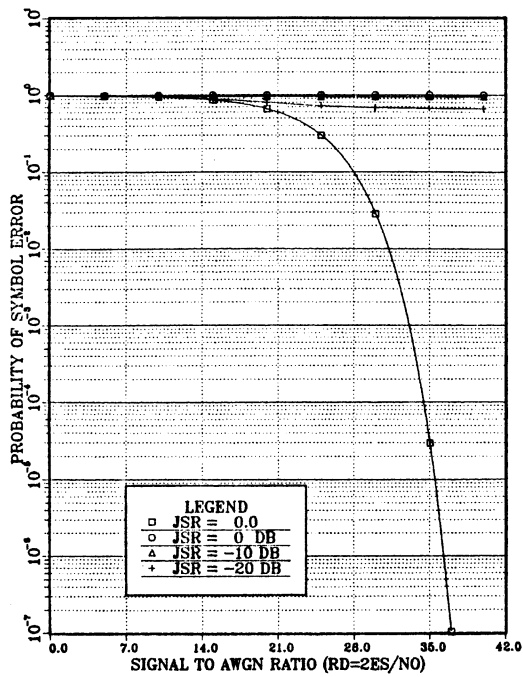


FIGURE 8 256-QAM PERFORMANCE IN JAMMING

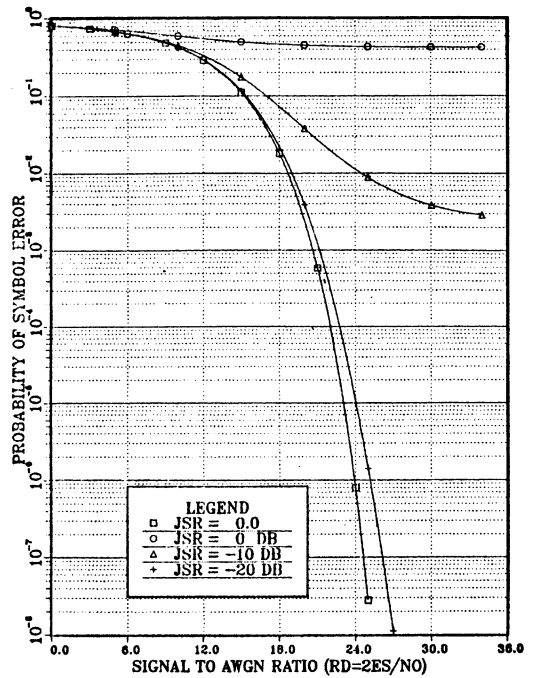


FIGURE 6 16-QAM PERFORMANCE IN JAMMING